



## Methanolic Extract of *Salvia Officinalis* plant as a green inhibitor for the corrosion of carbon steel in 1 M HCl

H. Bourazmi<sup>1</sup>, M. Tabyaoui<sup>1\*</sup>, L. EL Hattabi<sup>1\*</sup>, Y. El Aoufir<sup>1,2</sup>, M. Taleb<sup>3</sup>

<sup>1</sup> Laboratory of Nanotechnology, Materials & Environment, Faculty of Sciences, Mohammed V University, Rabat, Morocco

<sup>2</sup> Laboratory of Separation Processes, Faculty of Sciences, University Ibn Tofail, Kenitra, Morocco

<sup>3</sup> Laboratory of electrochemistry, modification and environment engineering, Faculty of Sciences USMBA Fes, Morocco

Received 05 May 2017,

Revised 14 Oct 2017,

Accepted 16 Oct 2017

### Keywords

- ✓ Corrosion ;
- ✓ Carbon steel ;
- ✓ Inhibitor ;
- ✓ *Salvia Officinalis*;
- ✓ Impedance ;
- ✓ Polarization curves ;

M. Tabyaoui

[hamidtabyaoui@yahoo.fr](mailto:hamidtabyaoui@yahoo.fr)

L. El Hattabi

[Latifa.elhattabi@gmail.com](mailto:Latifa.elhattabi@gmail.com)

### Abstract

The corrosion inhibition properties of methanolic extract of *Salvia Officinalis* (MESO) on carbon steel in hydrochloric acid (1 M HCl) solution has been examined and characterized by weight loss, Tafel polarization and electrochemical impedance spectroscopy (EIS) methods. These methods were complemented with SEM and EDX examinations of the electrode surface. The experimental results reveal that the inhibitor has a good inhibiting effect on the carbon steel in 1 M HCl solution. The protection efficiency increases with increasing inhibitor concentration, but the temperature decrease the effect on the inhibition efficiency of MESO. The adsorption of MESO is found to obey the Langmuir adsorption isotherm. Thermodynamic data show that the adsorption mechanism of MESO on carbon steel surface in 1 M HCl solution is probably electrostatic-adsorption. Potentiodynamic polarization studies have shown that MESO acts as a mixed type of inhibitor.

## 1. Introduction

Currently, carbon steel is extensively used in industrial equipment such as tanks, heat exchangers, acid pickling, industrial cleaning, acid descaling, oil well acid in oil recovery and the petrochemical processes, distillation tower and pipelines, where they are in contact with corrosive acids as hydrochloric acid [1-5]. Presently, the study of carbon steel corrosion phenomena undergoes all industrial applications of acid solutions. Generally, all acids are more aggressive, which is caused the increase in the dissolution of metals, in order to reduce this problem, the use of inhibitors organic containing nitrogen, oxygen and/or Sulphur atoms, heterocyclic compounds and  $\pi$ - electrons, are the most practical methods for protection against corrosion [6]. In the other hand, the organic compound can be adsorbed on the metal surface by its polar functions in order to form a protective layer as a barrier, isolating the metal from the corrosion [7]. Most synthetic organic inhibitors are widely more toxic to the environment and this has prompted the search for finding eco-friendly corrosion inhibitors [8-11]. Nowadays, the use of extract of different parts of plants as corrosion inhibitor in various environments has been an interesting subject for many researchers [12-14]. El Bribri and al. [9] investigated the corrosion inhibition of carbon steel in hydrochloric acid solution by *Euphorbia falcata* extract as eco-friendly inhibitor.

Moreover, Boumhara and al. [10] investigated the inhibition behavior of *Artemisia Mesatlantica* essential oil on the corrosion rate of carbon steel in 1 M HCl solution media, they found out this compound was adsorb on the steel surface and improved its corrosion behavior. The plant extracts include several chemical compounds as terpenes, phenolic compounds (such as tannins and flavonoids) and nitrogenous compounds (such as alkaloids, non-protein amino acids and glycoside) [15-18]. The aim of this study to find, environmentally friendly, non-toxic natural compound that could be used for acid pickling of carbon steel in acid medium, *Salvia officinalis* collected from sale (Morocco), was selected for this study.

The effect of concentration on the corrosion rate was investigated. Both kinetic and standard thermodynamic parameters were calculated and discussed in details by polarization method. also this paper reports the detailed study of the inhibition effect of the methanolic extract of *Salvia officinalis* (MESO) on the corrosion behaviour of carbon steel in normal hydrochloride solution (1M HCl) using gravimetric, polarization

and ac impedance methods. Adsorption isotherm, Scanning Electron Microscopy (SEM) and EDX have been applied to study the mechanism of carbon steel corrosion inhibition of this methanolic extract in acidic medium.

## 2. Experimental details

### 2.1. Preparation of solution

First of all, the hydrochloric acid solution was prepared by dilution of analytical grade 37% HCl with double distilled water. The solution tests are freshly prepared before each experiment by adding the inhibitor directly to the corrosive solution.

### 2.2. Plant material

The aerial parts of *Salvia officinalis* were collected in mars 2013 in the region of Sale (Morocco). A specimen was put down in the herbarium at the Faculty of Sciences in Rabat (Morocco). The dried plant material is stored in the laboratory at room temperature (298 K) before extraction.

### 2.3. Extract of *Salvia officinalis*

The selected plant *Salvia officinalis* was air dried at room temperature for two weeks, was then extracted with methanol using Soxhlet apparatus for about 8 h at a temperature not exceeding the boiling point of the solvent. The extract was evaporated to dryness using rotary evaporator at not more than 40 °C.

### 2.4. Materials

Corrosion tests were performed on carbon steel (Euro norm: C35E carbon steel and US specification: SAE 1035) of the following percentage composition (in wt %) of 0.370 % C, 0.230 % Si, 0.680 % Mn, 0.016 % S, 0.077 % Cr, 0.011 % Ti, 0.059 % Ni, 0.009 % Co, 0.160 % Cu and the remainder iron (Fe). Prior to each experiment, the carbon steel electrodes were first briefly ground with different grades of emery paper (120, 400, 800, 1000 and 1200) and washed thoroughly with distilled water and degreased with acetone.

### 2.5. Weight loss measurements

Rectangular specimens of carbon steel with dimensions 0.3cm ×1cm ×2 cm were used for weight loss measurements. The cleaned and dried specimens were weighed before immersion into the test solutions of 1M HCl. Tests were conducted with different concentrations of inhibitor. After immersion period (6 h), the specimens were washed with distilled water and degreased with ethanol. The experiments were tripled in each case and the mean values reported.

### 2.6. Potentiodynamic polarization measurements

Electrochemical measurements, including potentiodynamic polarization (PDP) and electrochemical impedance spectroscopy (EIS) methods were performed in a three-electrode cell. Carbon steel specimen was used as the working electrode (WE), a platinum wire as the counter electrode (CE) and a saturated calomel electrode (SCE) as the reference electrode (RE). The working electrode was prepared from carbon steel, mounted in resin epoxy, and the area exposed to solution was 1 cm<sup>2</sup>. The experiments were conducted in 100 ml of 1 M HCl solutions without and with 0.3; 0.6; 1.2 and 1.8 g/L of MESO at various temperatures 30, 40, 50 and 60°C. The polarization curves were obtained between potential ranges from -800 to -300 mV with scan rate of 1 mV/s. The electrochemical experiments were performed using a potentiostat Volta lab PGZ 301 coupled to a computer equipped with “Volta Master 4” software. The period of immersion sufficient to attain a stable value of  $E_{\text{corr}}$  is 30 min. All potentials were measured versus SCE. A schematic of the electrochemical cell setup is shown in Fig. 1.

### 2.7. EIS study

The EIS measurements were carried out in each case just after the acquisition of the polarization curve. Impedance diagrams were obtained in the frequency range between 100 kHz and 10 mHz with ten points per decade using a 10 mV peak-to-peak sinusoidal voltage. The above procedures were repeated three times with success for each concentration of the tested plant extract. The impedance data were analyzed and fitted using graphing and analyzing impedance software, version EC-Lab V 9.97.

### 2.8. SEM–EDX analysis

The surfaces of the carbon steel samples after exposure to hydrochloric acid in the absence and presence of MESO were examined by scanning electron microscopy coupled with energy dispersive X-ray (SEM/EDX) spectroscopy. In order to get insights about the morphological changes occurred on the surface before and after

the addition of inhibitors using SEM–EDX analysis, the addition of inhibitors using SEM–EDX analysis. The different rectangular specimens of carbon steel having dimensions 0.3 cm × 1 cm × 2 cm. The cleaned and dried specimens were weighed before immersion into the of hydrochloric acid solution as mentioned in weight loss tests. The specimens were immersed for 6h in the absence and presence of optimum concentration of the inhibitor at room temperature.

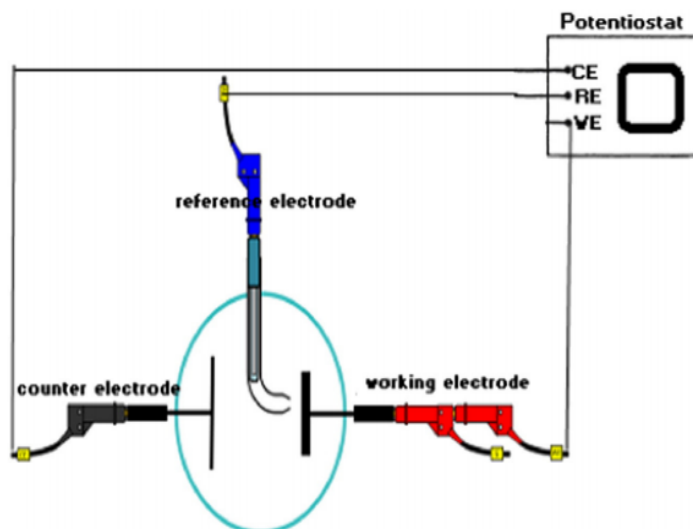


Figure 1: A schematic of the electrochemical cell setup

### 3. Results and discussion

#### 3.1. Potentiodynamic polarization study

The effect of the MESO on the behaviors of anodic and cathodic polarization curves of carbon steel in 1M HCl solution at 30 °C was studied by polarization measurements are shown in Figure 2. The kinetic parameters including corrosion current density ( $I_{corr}$ ), corrosion potential ( $E_{corr}$ ), cathodic Tafel slope ( $\beta_c$ ), and anodic Tafel slope ( $\beta_a$ ) are regrouped in Table 1. The  $I_{corr}$  was determined by Tafel extrapolation. The  $I_{corr}$  values were used to calculate the inhibition efficiency,  $\eta_{Tafel}$  (%), using the following equation [19]:

$$\eta_{Tafel} (\%) = \frac{I_{corr} - I_{corr(i)}}{I_{corr}} \times 100 \quad (1)$$

Where  $I_{corr}$  and  $I_{corr(i)}$  are the corrosion current densities for steel electrode in the uninhibited and inhibited solutions, respectively.

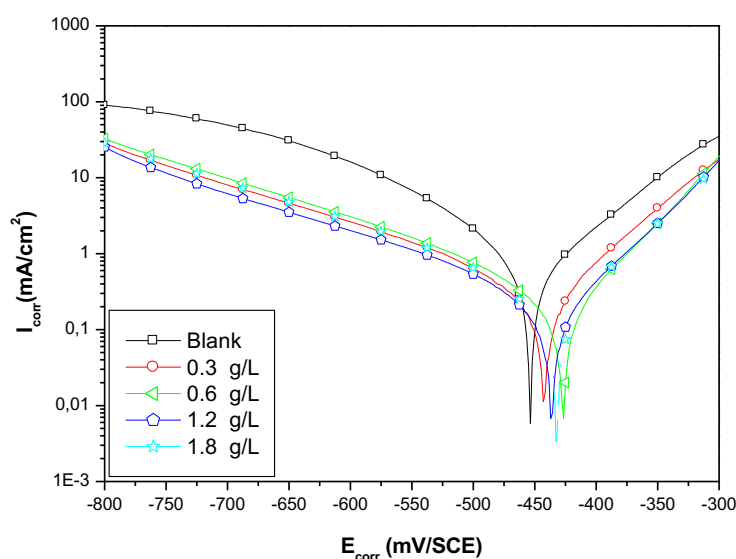


Figure 2: Potentiodynamic polarization curves for carbon steel in 1 M HCl at various concentrations of MESO at 303 K

**Table 1:** Potentiodynamic polarization parameters for carbon steel in 1 M HCl at various concentrations of MESO at 303K

Concentration (g/L)	$-E_{\text{corr}}$ vs. SCE(mV)	$I_{\text{corr}}$ ( $\mu\text{A cm}^{-2}$ )	$-\beta_c$ ( $\text{mV dec}^{-1}$ )	$\beta_a$ ( $\text{mV dec}^{-1}$ )	$\eta_{\text{Tafel}}$ (%)
Blank	453	890	114	99	-
0.3	442	187	112	69	79
0.6	426	138	100	60	85
1.2	434	126	111	64	86
1.8	432	121	94	62	86

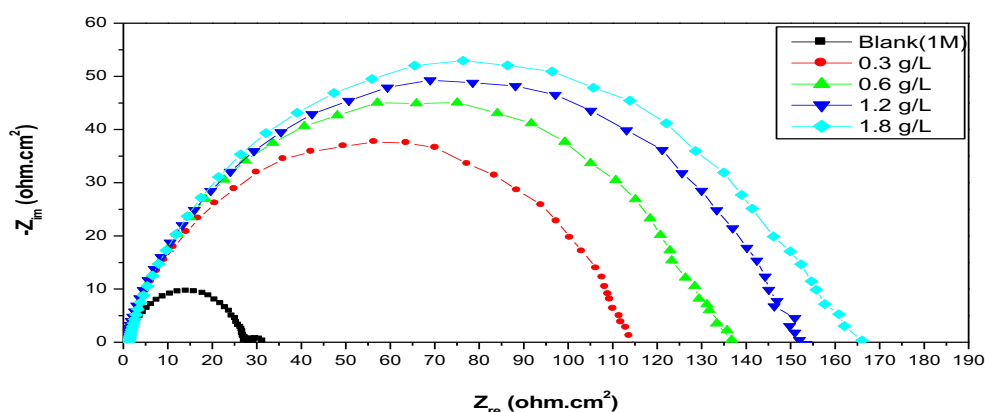
It is illustrated from Figure 2 that both anodic metal dissolution of iron and cathodic hydrogen evolution reaction were inhibited after the addition of MESO to 1 M HCl solution. The inhibition of these reactions was more pronounced on increasing MESO concentration. From Table 1, it is clear that the values of  $I_{\text{corr}}$  decrease considerably with the increase of the concentration of MESO, however, there is slight variation of corrosion potential ( $E_{\text{corr}}$ ) in presence of different concentration of inhibitor. The shifting of the corrosion potentials of carbon steel in presence of the tested inhibitor, are in the range of 10.5 – 27 mV anodically compared to the uninhibited solution and in literature, if the displacement in  $E_{\text{corr}}$  in presence of inhibitor tested is greater than 85 mV with respect to corrosion potential of the blank [20], the inhibitor may then be classified as cathodic or anodic type and if the displacement is less than 85 mV, then the inhibitor may be regarded as mixed-type. In our study, the obtained results indicated that MESO acts as mixed-type inhibitor with anodic predominant.

The parallel cathodic Tafel lines (figure 2) and the low variation of the constant cathodic Tafel slopes  $\beta_c$  (Table 1) suggest that the cathodic process "the hydrogen evolution reaction" is activation controlled. The addition of MESO to the 1 M HCl solution did not modify the hydrogen evolution mechanism and the reduction of  $\text{H}^+$  ions at the steel surface takes place mainly by a charge transfer mechanism. The MESO molecules are adsorbed onto the carbon steel surface for block the reaction sites cathodic and anodic of the steel surface. In this way, the reduce of the  $\text{H}^+$  ions is decreased while the actual reaction mechanism remains unaffected [21]. The decrease in anodic and cathodic current densities during the increase the MESO concentration showed that corrosion rate of carbon steel decreased on increasing MESO concentration. The corrosion inhibition efficiency ( $\eta_{\text{Tafel}}(\%)$ ) calculated by equation (1) increases with MESO concentration reaching its maximum value at 1.8 g/L.

### 3.2. Method EIS

The corrosion inhibition property of MESO on carbon steel was examined by EIS technique. Figures 3 and 4 show the Nyquist and Bode diagrams of carbon steel obtained at open-circuit potential after 30 min of immersion in 1 M HCl solution in the absence and presence of different concentrations of MESO. The Nyquist diagrams present one capacitive loop with one capacitive time constant in the Bode-phase plots, as illustrated in figures 3 and 4, which confirms that only one phenomenon produced.

The capacitive loop is related to the charge transfer process of the metal corrosion and double layer behaviour.

**Figure 3:** Nyquist diagrams for carbon steel in 1 M HCl containing different concentrations of MESO at 303 K

Each shape of the diagrams (Nyquist and Bode) is very similar in absence and presence all concentrations tested, these results indicate that the addition of the inhibitor no change in the corrosion mechanism [22]. Analysis of the figure 3 shows that, the Nyquist diagrams are larger in presence of inhibitor as compared to the

blank solution. The diameters of capacitive loop increase with a rise in MESO concentration is the result of the adsorption of the inhibitor on the carbon steel surface [23], consequently the protection efficiency increases.

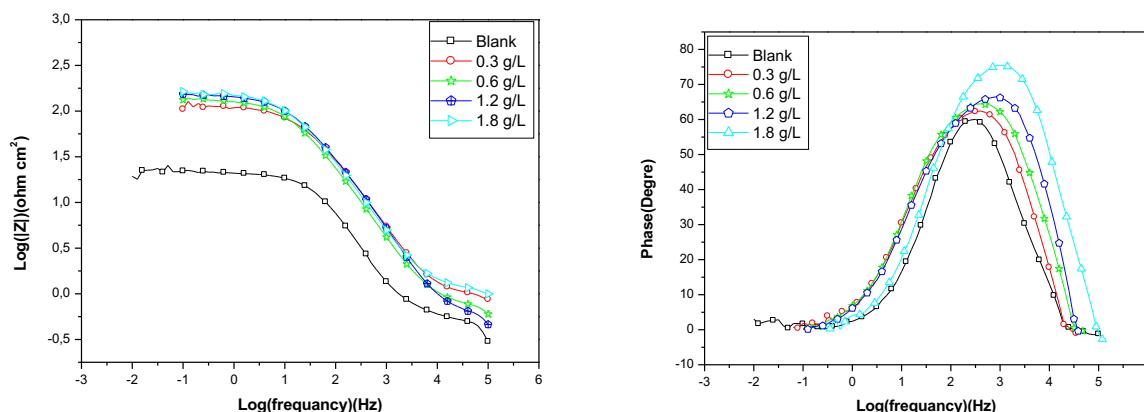


**Figure 4:** Bode diagrams for carbon steel in 1 M HCl containing different concentrations of MESO at 303 K

**Table 2:** Impedance parameters and inhibition efficiency values for carbon steel in 1 M HCl containing different concentrations of MESO at 303 K

Concentration (g/L)	$R_s$ ( $\Omega \text{ cm}^2$ )	$R_{ct}$ ( $\Omega \text{ cm}^2$ )	$10^4 A$ ( $\Omega^{-1} \text{ s}^n \text{ cm}^{-2}$ )	$n$	$C_{dl}$ ( $\mu\text{F cm}^{-2}$ )	$\tau_d$ (mS)	$\eta_{EIS} \%$	$\Theta$
Blank	0.573 5	20	2.450	0.850 9	96.721	1.962	-	-
0.3	0.947 8	107	1.768	0.784 5	59.555	6.414	81	0.8130
0.6	0.754 6	129	1.523	0.778 1	49.733	6.450	85	0.8449
1.2	0.459 1	148	1.482	0.759 1	44.124	6.543	87	0.8648
1.8	1.0360	155	1.306	0.766 2	39.729	6.158	87	0.8709

The Nyquist plots illustrated in figure 3, are not perfect semicircle, this phenomenon often referred to as frequency dispersion, can be attributed to inhomogeneity and roughness or interfacial phenomena in the solid surface [24].

The developed of physical model is essential to fit the experimental data and extract the parameters which characterize the corrosion process. Figure 5 shows the equivalent circuit model used to fit the experimental impedance data of carbon steel in presence of 1 M HCl alone and with 1M HCl containing MESO.

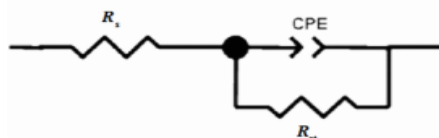


**Figure 5:** Equivalent circuit model used to fit the EIS data

In this case  $R_s$  refers to the solution resistance, CPE the constant phase element,  $R_{ct}$  the charge transfer resistance. The parameters are collected in Table 2; while the double layer capacitance ( $c_{dl}$ ) values are calculated using the Eq. (2):

$$c_{dl} = \sqrt[n]{Q \cdot R_{ct}^{1-n}} \quad (2)$$

Where  $Q$  is the magnitude of CPE (in  $\Omega^{-1} \text{ s}^n \text{ cm}^{-2}$ ),  $n$  is an exponent related to the phase shift ( $0 \leq n \leq 1$ ) and can be used as a measure the deviation from the ideal capacitive behavior due to the surface irregularity [25]. The Eq. (3) was used to calculate the  $\eta_{EIS} \%$ :

$$\eta_{EIS} \% = \frac{R_{ct} - R_{ct}^i}{R_{ct}} \times 100 \quad (3)$$

Where  $R_{ct}$  and  $R_{ct}^i$  are the charge transfer resistance values in with and without MESO, respectively. The relaxation time constant ( $\tau_d$ ) of charge-transfer process was calculated by equation (4):

$$\tau_d = C_{dl} R_{ct} \quad (4)$$

The table 2 clearly shows that in whole concentration tested, the charge transfer resistance values ( $R_{ct}$ ) increase with increasing of MESO concentration, which explains better inhibition effect, is obtained. The variation simultaneous of the  $R_{ct}$  is related with decrease of the double-layer capacitance ( $C_{dl}$ ). This effect is connected with simultaneous decrease of the double-layer capacitance ( $C_{dl}$ ), these results can be demonstrate, by the formation of an insulating protective film [26], due to the adsorption of organic molecules on electrode surfaces [27]. This data can be explained by reduction of surface inhomogeneity due to the adsorption of the inhibitor on the most active sites. On the other hand, the calculated value of time constant  $\tau$  obtained in the addition of MESO results in an increase in  $\tau$  value at 1.2 g/ L ( $\tau = 6,543$  mS) and a slight decrease at 1.8 g/ L ( $\tau = 6,158$  mS) compared to the uninhibited solution ( $\tau = 1,962$  mS).

Generally, the simultaneous decrease in  $C_{dl}$  indicated in table 2 is explained by a decrease in local dielectric constant and/or an increase in the thickness of a protective layer at electrode surface, enhancing therefore the corrosion resistance of the studied steel [28]. This trend is in accordance with Helmholtz model, given by the following equation [29]:

$$c_{dl} = \frac{\epsilon\epsilon_0}{d} \quad (5)$$

In addition, previous works [30,31] show that the Plant extracts containing a mixture of various compounds such as hydroxycinnamic acid, flavonols, phenolic compounds, and hydroxyl benzoic acid are present important inhibition efficiency to keep the environment greener, which further confirm the advantage of using MESO as a corrosion inhibitor.

### 3.3. Weight loss measurements

The effect of addition of inhibitor tested at different concentrations on the corrosion of carbon steel in 1 M HCl solution was studied by weight loss method at 303 K after 6 h of immersion period. The corrosion rate ( $C_R$ ) and inhibition efficiency  $\eta_{WL}(\%)$  were calculated according to the Eqs (6) and (7) [32,33], respectively:

$$C_R = \frac{W_b - W_a}{At} \quad (6)$$

$$\eta_{WL}(\%) = \left(1 - \frac{W_i}{W_0}\right) \times 100 \quad (7)$$

Where  $W_b$  and  $W_a$  are the specimen weight before and after immersion in the tested solution,  $w_0$  and  $w_i$  are the values of corrosion weight losses of the carbon steel due to the dissolution in studied aggressive medium without and with the studied range of the MESO concentrations, respectively, A the total area of the carbon steel specimen ( $cm^2$ ) and t is the exposure time (h). After the analysis of the table 3, we notice that the MESO inhibits the corrosion of carbon steel at all concentrations used in this study. The variation of  $C_R$  and  $\eta_{WL}(\%)$  with the MESO concentration are shown in Figure 6.

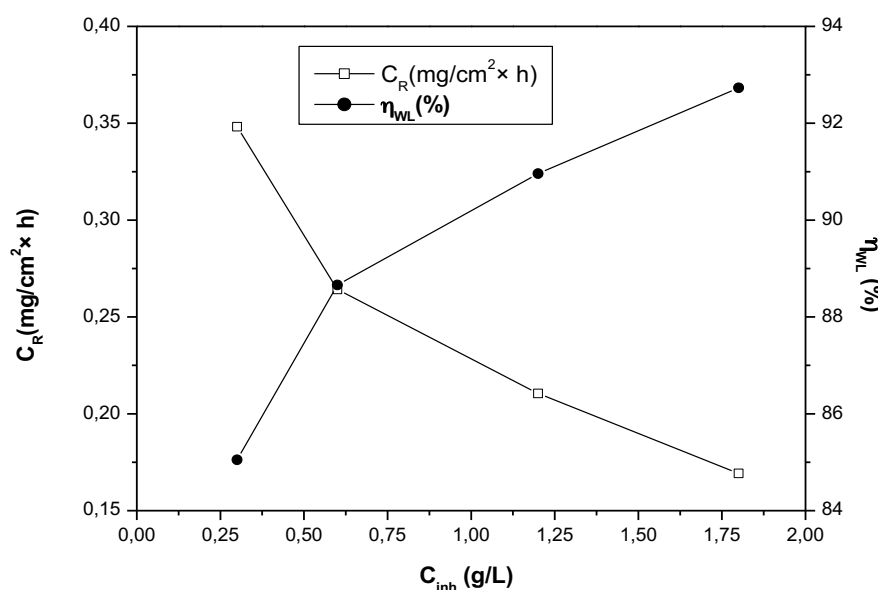


**Figure 6:** Variation of corrosion rate and inhibition efficiency of carbon steel in 1 M HCl containing various concentrations of MESO at 303 K

It can be remarked from Table 3, that the MESO inhibits the corrosion of the carbon steel and the inhibition efficiency  $\eta_{WL}(\%)$  increases with increasing inhibitor concentration. The values of  $\eta_{WL}\%$  are little higher than those obtained by the electrochemical techniques which may be due to the length immersion time resulting strong and stable adsorption. The presence of the organic compounds containing in the Plant extracts such as hydroxycinnamic acid, flavonols and phenolic, improve the electron release power which produces high inhibition efficiency. The values of inhibition efficiency obtained in three techniques (EIS, PDP and WL) are in good agreement.

**Table 3:** Weight loss data of carbon steel in 1M HCl for various concentration of the MESO at 303 K

Concentration (g/L)	$W_{corr}$ ( $mg/cm^2 \times h$ )	$\eta_{WL}$ (%)
Blank	2.3301	-
0.3	0.3482	85
0.6	0.2642	89
1.2	0.2105	91
1.8	0.1692	93

### 3.4. Effect of temperature

The effect of temperature on the corrosion inhibition property of the MESO was studied in 1M HCl in the absence and in the presence of 1.8 g/L of inhibitor during 30 min of immersion by potentiodynamic polarization (Figure 7). The analysis of the obtained data, summarized in Table 4 and illustrated in Figure 7, clearly shows a rise of corrosion current densities ( $I_{corr}$ ) with the increase of temperature and it is more augmented for uninhibited solution (1M HCl).

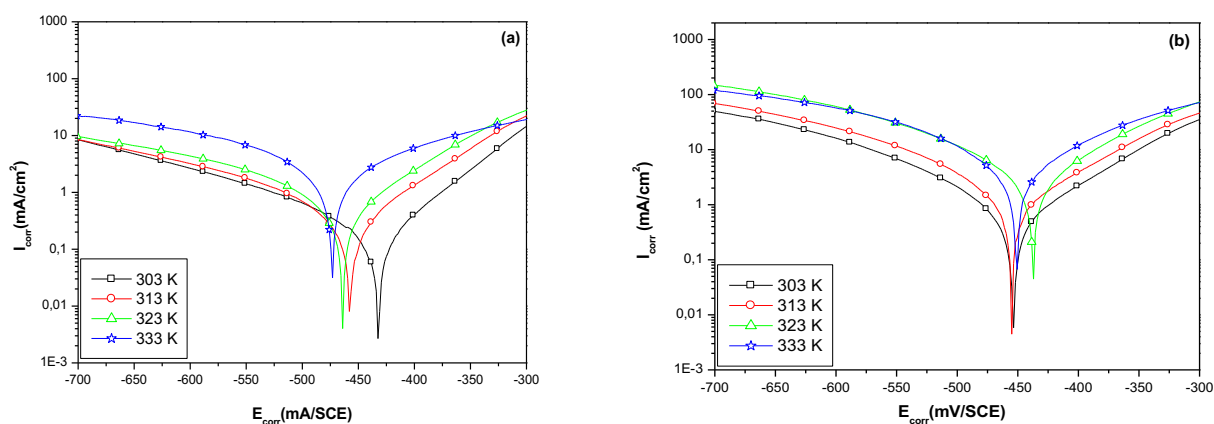


**Figure 7:** Potentiodynamic polarization curves for steel in 1M HCl at various temperatures in the absence and in the presence of 1.8 g/L of inhibitor

**Table 4:** Temperature influence on the PDP parameters for carbon steel in 1M HCl with and without 1.8 g/L of MESO at 303 K.

Inhibitor	Temperature (K)	$-E_{corr}$ vs. SCE (mV)	$I_{corr}$ ( $\mu A cm^{-2}$ )	$-\beta_c$ ( $mV dec^{-1}$ )	$\beta_a$ ( $mV dec^{-1}$ )	$\eta_{Tafel}$ (%)
Blank	303	453	890	114	99	-
	313	454	981	106	83	-
	323	443	1580	85	91	-
	333	449	1910	63	60	-
MESO	303	432	121	94	62	86
	313	456	260	104	79	74
	323	463	474	126	87	70
	333	473	665	56	57	65

We note that the inhibition efficiency depends on the temperature because its value decreases progressively with the increase of the temperature. These results can be explained by the decrease of the strength of the adsorption process at high temperature, these results can suggest a physical adsorption mode, indicating that the increase of the temperature cause the rise of the dissolution of carbon steel, which slowed down adsorption of MESO at the

metal surface. The activation parameters for the corrosion process were calculated from Arrhenius type plot according to the following equations (Eqs. (8), (9)) [34]:

$$I_{corr} = A \exp\left(-\frac{E_a}{RT}\right) \quad (8)$$

$$I_{corr} = \frac{RT}{Nh} \exp\left(\frac{\Delta S_a^*}{R}\right) \exp\left(-\frac{\Delta H_a^*}{RT}\right) \quad (9)$$

Where  $E_a$  is the apparent activation corrosion energy,  $R$  is the universal gas constant,  $A$  is the Arrhenius pre-exponential factor,  $h$  is Plank's constant,  $N$  is Avogrado's number, is the entropy of activation and  $\Delta H_a^*$  is the enthalpy of activation.

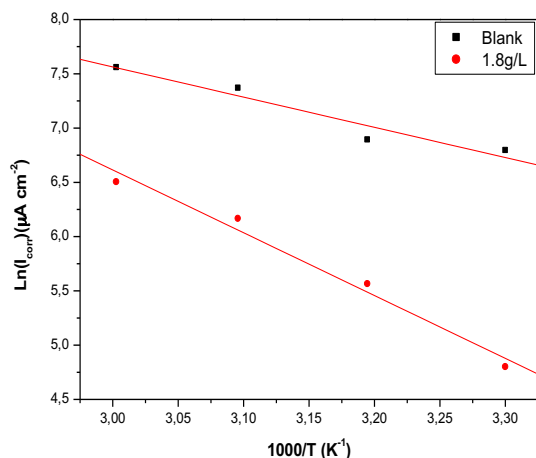


**Figure 8:** Arrhenius plots of steel in 1 M HCl with and without 1.8 g/L MESO

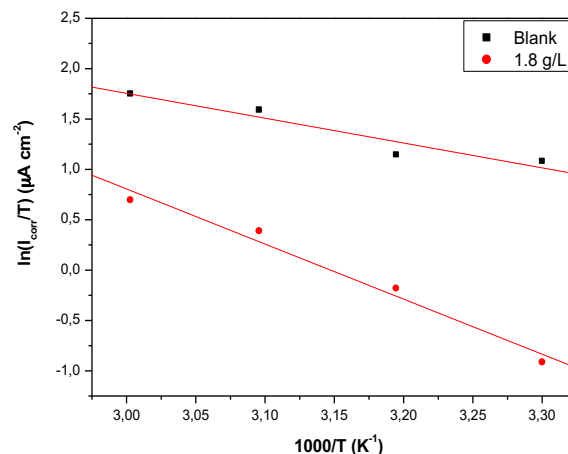


**Figure 9:** Variation of  $\ln(I_{corr} / T)$  versus  $1000/T$  for blank and 1 M HCl + 1.8 g/L of MESO

The apparent activation energy was determined from the slopes of  $\ln(I_{corr})$  vs  $1/T$  graph given in Figure 8 a plot of  $\ln(I_{corr}/T)$  against  $1/T$  (Figure 9) gave a straight line with slope  $(\Delta H_a^*/R)$  and intercept  $(\ln(R/Nh) + (\Delta S_a^*/R))$ , from which the values of  $\Delta H_a^*$  and  $\Delta S_a^*$  were calculated and listed in Table 5.

The activation energy ( $E_a$ ) increase in the presence of inhibitor compared to the blank solution suggests that inhibitor tested can be considered as physically adsorbed on the electrode surface, knowing that if energy of activation of the inhibitor solution unchanged or lower compared with blank medium suggest chemisorption [35]. The table 5 clearly shows that, the  $E_a$  values increased progressively after the addition of the inhibitor, these results suggest that the adsorption of the inhibitor on the carbon steel is probably considered as physical adsorption.

**Table 5:** The value of activation parameters for steel in 1M HCl in the absence and presence of 1.8g/L of MESO

	$E_a$ (kJ mol <sup>-1</sup> )	$\Delta H_a^*$ (kJ mol <sup>-1</sup> )	$\Delta S_a^*$ (kJ mol <sup>-1</sup> )
Blank	-23.150	20.511	-121.416
1.8 g/L	-48.116	45.477	-54.411

After the analysis of the activation parameters ( $\Delta S_a^*$  and  $\Delta H_a^*$ ) regrouped in the table 5 we note that, the positive signs of  $\Delta H_a^*$  explain the endothermic nature of carbon steel dissolution process meaning that dissolution of the electrode is difficult [36]. It is clear from Table 5 that the entropy of activation ( $\Delta S_a^*$ ) in the presence of MESO are higher than in the absence of inhibitor. The increase of  $\Delta S_a^*$  is generally interpreted as an increase in disorder. This behavior can be explained as a result of the replacement process of water molecules during adsorption of MESO on the steel surface [37].

### 3.5 Adsorption isotherm

The adsorption isotherm experiments were effected for describes the molecular interaction between the inhibitor molecules and the active sites on the carbon steel surface. In order to evaluate the adsorption process of MESO in carbon steel surface, Langmuir, Temkin, Freundlich and Frumkin adsorption isotherms were tested. The degree of surface coverage ( $\theta$ ) for tested MESO was calculated from EIS method. A plot of  $(C_{inh}/\theta)$  versus

( $C_{inh}$ ) (figure 10) was found to be the best fit which suggests that adsorption of the MESO on carbon steel surface in test medium obeys the Langmuir adsorption isotherms. The Langmuir isotherms can be best expressed by following relation (10):

$$\frac{C_{inh}}{\theta} = \frac{1}{K_{ads}} + C_{inh} \quad (10)$$

The degree of surface coverage ( $\theta$ ) was illustrated in Table 2 and calculated according to the following equation:

$$\theta = \frac{R_{ct} - R_{ct}^i}{R_{ct}} \quad (12)$$

Where  $R_{ct}$  and  $R_{ct}^i$  are the charge transfer resistance values without and with addition of inhibitor, respectively.

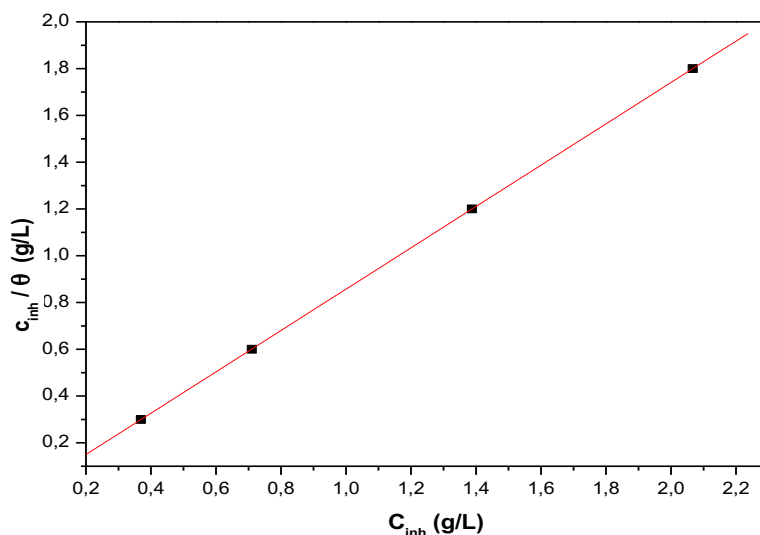


**Figure 10:** Langmuir adsorption plots for carbon steel in 1 M HCl containing different concentration of MESO at 303K

**Table 6:** Langmuir adsorption parameters for carbon steel in 1M HCl containing different concentration of MESO at 303K

Slope	Intercept	$K_{ads}$	Regression coefficient ( $R^2$ )
0.02674	0.88384	1.13143	0.9999

The value of the regression coefficient ( $R^2= 1$ ) confirms that this inhibitor (MESO) obey the Langmuir adsorption isotherm with 1.0 M HCl medium. This indicates the inhibition behavior is attributed to the electrostatic interaction between the organic molecules and carbon steel surface. It is very important to note that the discussion on the behavior of the adsorption isotherm using natural product extracts as inhibitors in terms of thermodynamics (such as the standard free energy of the adsorption value ( $\Delta G_{ads}$ )) are not possible [38,39].

### 3.6. SEM-EDS analysis

Figure 11 shows SEM micrographs of carbon steel immersed in 1 M HCl in the absence and presence of 1.8 g/L plant extract. The SEM image (Figure 11a) of the carbon steel specimen in the absence of the plant extract shows an irregular and damaged surface owing to the attack of acid. The micrograph of the inhibited carbon steel specimen (Figure 11b) shows a relatively smooth surface protected by the adsorbed layer of the plant extract.

EDS is used to determine the elemental composition of carbon steel before and after the immersion of its surface. The EDS spectrum reported in Figures 11a' and b' showed the characteristic peaks of the specimen and a marked presence of Fe, O and C atoms in the absence and presence of the plant extract inhibitor. The figure 11b' present low peak of oxygen in compared with blank solution; this result confirmed the formation of the inhibitor film.

With these results, we confirmed that the high inhibition efficiency values obtained in the weight loss and the electrochemical measurements can be attributed to a good protective film formation on the surface of the carbon steel substrate.

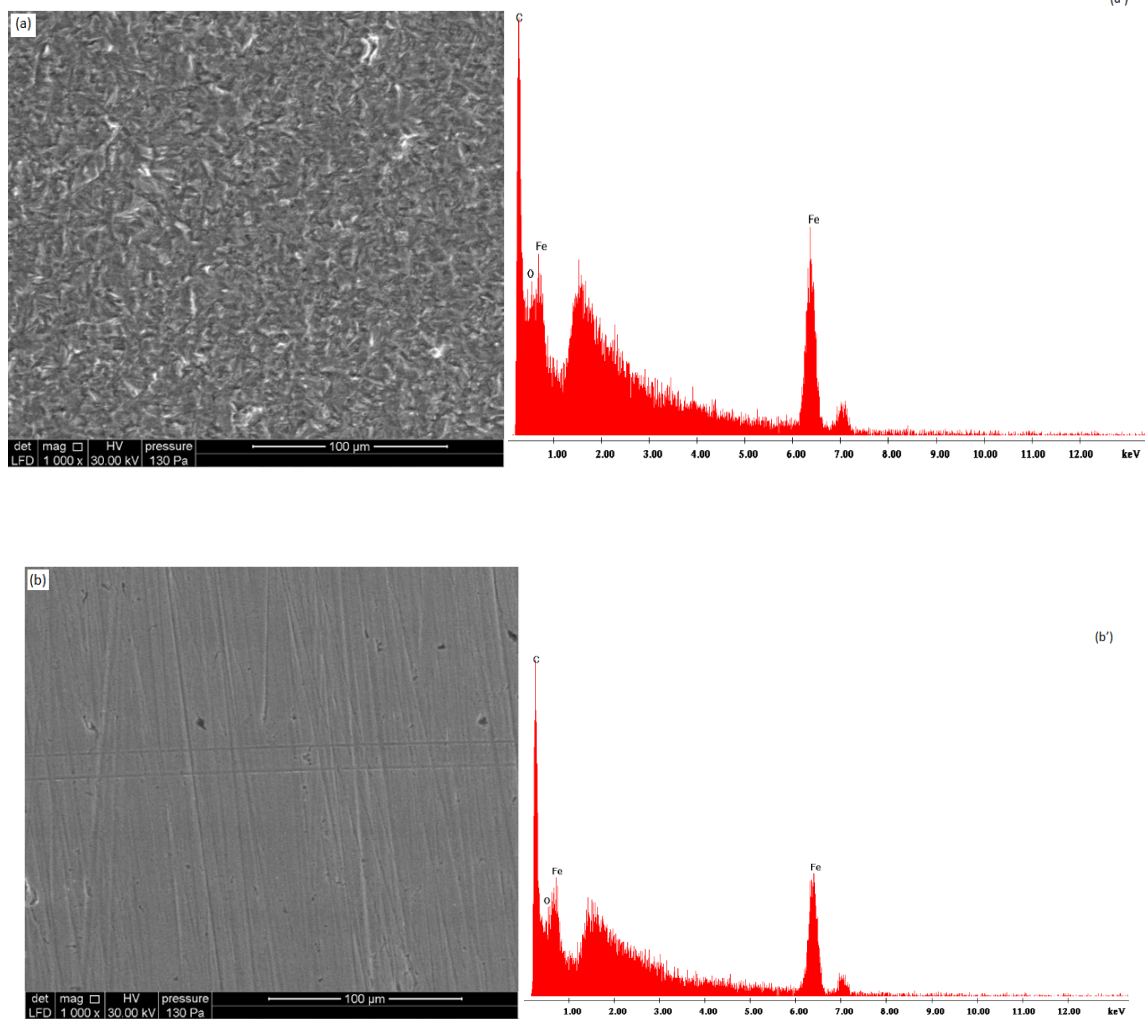


**Figure 11:** SEM images and EDX spectra of carbon steel in acidic solution after 6 h immersion in the absence (Figures 11: a, a') and in the presence (Figures 11: b, b') of 1.8g/L of MESO

## Conclusion

The following conclusions could be deduced:

- The MESO acts as a mixed inhibitor without modifying the hydrogen reduction mechanism.
- The inhibition efficiency increases with increased MESO concentration to attain a maximum value of 87 % at 1.8 g/L
- The inhibition efficiency of MESO decreases with the rise of temperature.
- Adsorption of inhibitor tested follows Langmuir adsorption isotherm.
- The presence of MESO increases the activation energy of the corrosion process.
- The inhibitor was physically adsorbed on the steel surface.

## References

1. P. Altoe, G. Pimenta, C.F. Moulin, S.L. Diaz, O.R. Mattos, *Electrochim. Acta.* 41 (1996) 1165.
2. R. Cabrera-Sierra, I. Garcia, E. Sosa, T. Oropeza, I. Gonzalez, *Electrochim. Acta.* 46 (2000) 487.
3. M.A. Amin, M.M. Ibrahim, *Corros. Sci.* 53 (2011) 873.
4. P.M. Dasami, K. Parameswari, S. Chitra, *Measurement.* 69 (2015) 195.
5. A.H. Ostovari, S.M. Peikari, S.R. Shadizadeh, S.J. Hashemi, *Corros. Sci.* 51 (2009) 1935.
6. I. Ahamad, R. Prasad, M.A. Quraishi, *Corros. Sci.* 52 (2010) 1472.
7. E.E. Ebenso, *Bull. Electrochem.* 19 (2003) 209.
8. R. Fdil, M. Tourabi, S. Derhali, A. Mouzdahir, K. Sraidi, C. Jama, A. Zarrouk, F. Bentiss, *J. Mater. Environ. Sci.* 9 (1) (2018) 358.
9. A. El Bribri, M. Tabyaoui, B. Tabyaoui, H. El Attari, F. Bentiss, *Mat.Chem.Phys.* 141 (2013) 240.

10. K. Boumhara, M. Tabyaoui, C. Jama, F. Bentiss, *J. Ind. Eng. Chem.* 29 (2015) 146.
11. L. El Hattabi, J. Costa, M. Desjobert, A. Guenbour, M. Tabyaoui, *Mor. J. Chem.* 4 (4) (2016) 862.
12. J. P. Rajan, R. Shrivastava, R. K. Mishra, *Prot. Met. Phys. Chem.* 12 (1) (2018) 2070.
13. F. El Hajjaji, H. Greche, M. Taleb, A. Chetouani, A. Aouniti, B. Hammouti, *J. Mater. Environ. Sci.* 7 (2016) 567.
14. A. Batah, M. Belkhaouda, L. Bammou, A. Anejjar, R. Salghi, A. chetouani, L. Bazzi, B. Hammouti, *Mor. J. Chem.* 5 (4) (2017) 580.
15. M.A. Amin, M.M. Ibrahim, *Corros. Sci.* 53 (2011) 873.
16. P.C. Okafor, M.E. Ikpi, I.E. Uwah, E.E. Ebenso, U.J. Ekpe, S.A. Umoren, *Corros. Sci.* 50 (2008) 2310.
17. J. Dubey, N. Jeengar, R.K. Upadhyay, A. Chaturvedi, *J. Rec. Sci.* 1 (2012) 73.
18. S. Banerjee, V. Srivastava, M.M. Singh, *Corros. Sci.* 59 (2012) 35.
19. A. Zarrouk, B. Hammouti, T. Lakhlifi, M. Traisnel, H. Vezin, F. Bentiss, *Corros. Sci.* 90 (2015) 572.
20. E.S. Ferreira, C. Giancomelli, F.C. Giacomelli, A. Spinelli, *Mater. Chem. Phys.* 83 (2004) 129.
21. K. Khaled, *Acta.* 48 (2003) 2493.
22. F.M. Reisde, H.G. Melo, I. Costa, *Acta.* 51 (2006) 1780.
23. R. Solmaz, *Corros. Sci.* 52 (2010) 3321.
24. H. Shih, F. Mansfeld, *Corros. Sci.* 29 (1989) 1235.
25. W. Chen, S. Hong, B. Xiang, H. Luo, *Corros. Eng. Sci. Technol.* 48 (2013) 98.
26. K. Krishnaveni, J. Ravichandran, *J. Electroanal. Chem.* 735 (2014) 24.
27. M. Outirite, M. Lagrenée, M. Lebrini, M. Traisnel, C. Jama, H. Vezin, F. Bentiss, *Electrochim. Acta.* 55 (2010) 1670.
28. M. Lebrini, M. Lagrenée, H. Vezin, M. Traisnel, F. Bentiss, *Corros. Sci.* 49 (2007) 2254.
29. C.H. Hsu, F. Mansfeld, *Corrosion* 57 (2001) 747.
30. M. Tiruvengadam, I.M. Chung, *Food. Chem.* 173 (2015) 185.
31. A.M.A. Gaber, B.A.A. El-Nabey, I.M. Sidahmed, A.M.E. Zayady, M. Saadawy, *Corros. Sci.* 48 (2006) 2765.
32. I. Ahamad, R. Prasad, M.A. Quraishi, *Corros. Sci.* 52 (2010) 933.
33. F. Bentiss, M. Outirite, M. Traisnel, H. Vezin, M. Lagrenée, B. Hammouti, S.S. AlDeyab, C. Jama, *Int. J. Electrochem. Sci.* 7 (2012) 1699.
34. R. Villamil, P. Corio, J. Rubim, S. Agostinho, *J. Electroanal. Chem.* 535 (2002) 75.
35. T. Tsuru, S. Haruyama, J. Gijutsu, *J. Jpn. Soc. Corros. Eng.* 27 (1978) 573.
36. H. Zarrok, A. Zarrouk, R. Salghi, B. Elmahi, B. Hammouti, S.S. Al-Deyab, M. Ebn Touhami, M. Bouachrine, H. Oudda, S. Boukhris, *Int. J. Electrochem. Sci.* 8 (9) (2013) 11474.
37. M.S. Morad, A.M. Kamal El-Dean, *Corros. Sci.* 48 (2006) 3398.
38. L. Valek, S. Martinez, *Mater. Lett.* 61 (2007) 148.
39. L. EL Hattabi, M. EL Moudane, H. Harhar, A. Bellaouchou, A. Ghanimi, A. Guenbour, J. Costa, J.M. Desjobert, M. Tabyaoui, *J. Mater. Environ. Sci.* 7 (9) (2016) 3162.

(2018) ; <http://www.jmaterenvirosci.com>